SMiRT-12 / K. Kussmaul (Editor)

BG11/1

AN INCREMENTAL FORMULATION OF THE MOVING-GRID FINITE ELEMENT METHOD FOR THE PREDICTION OF DYNAMIC CRACK PROPAGATION

H.M. Koh, H.S. Lee and U.Y. Jeong

Seoul National University, Seoul, Korea

ABSTRACT

This paper presents an incremental formulation of moving-grid finite element method which can predict both field variables and crack-tip speed simultaneously in unstable mode-I crack propagation problems. Energy balance equation is included as a fracture criterion in the governing equation of motion. The variational statement of the governing equation is derived based on the Eulerian-Lagrangian kinematic description and used for a basis of moving-grid finite element procedure suitable for a prediction of dynamic crack propagation. Computational aspects of the present method and prediction results of mode-I problems are discussed.

1. ANALYSIS METHODS FOR DYNAMIC FRACTURE PROBLEMS

The prediction of dynamic crack propagation and arrest behavior in brittle materials is an importance issue in many engineering problems. Since cracks propagate very rapidly in brittle materials, at speeds of the order of the material's characteristic wave speed, the dynamic crack growth can lead to catastrophic failure of some structures.

Analytic solutions for dynamic crack growth problems are limited to idealized geometries and loading conditions, so numerical methods are necessary to obtain solutions for realistic conditions. Among them, finite element method is a popular numerical method used for the analysis and prediction of the dynamic crack propagation [1, 7, 8, 14]. The question of how to model the crack propagation and its effects on geometry and field variables, however, has been one of the major issues in the analysis and prediction of dynamic crack propagation by the finite element method.

Three classes of modeling methods are available to simulate crack growth: node-release method, remeshing method and moving-grid method. The node-release and remeshing method are based on conventional Lagrangian kinematic description, and the moving-grid method on the mixed Eulerian-Lagrangian description.

(1) Node-release method : This method simulates crack growth by uncoupling paired nodes along the expected crack path [15], so that the crack advances one element edge at a time. The method does not describe continuous crack-tip

motion - the crack advances an entire element length at each step. This fact makes it very difficult to apply this method to problems of prediction of dynamic crack propagation because the crack-tip motion cannot be adjusted for a given time increment.

(2) Remeshing method : A new mesh is generated at each time step to represent the new crack configuration [1, 14]. The new mesh can or cannot maintain the topology of the old mesh. The crack growth model is still discontinuous as in the node-release method. However, the increment of crack growth is no longer constrained by the geometry of the old mesh. The interpolation of field variables to the new mesh locations introduces a source of error, because the new mesh cannot represent the solution computed on the old mesh exactly. This interpolation error is especially significant in the vicinity of crack-tip singularities.

(3) Moving-grid method : This method is based on the mixed Eulerian-Lagrangian description [6]. The method can model smooth crack-tip motion by a continuous variation of domain mappings. Most of the drawbacks of the node-release and remeshing methods can be eliminated by the moving-grid method. The method has been successfully applied to linear elastic fracture problems, elastodynamic fracture problems and crack growth problems in history-dependent materials.

2. FRACTURE ANALYSIS USING THE ELD MODEL

In the mixed Eulerian-Lagrangian description (ELD) [6, 10], a reference configuration is introduced in addition to usual material configurations as shown in Fig. 1a. While the material configuration varies with time, the reference configuration is set to be invariant with time. Time-dependent mapping is used to relate the two configurations. Finite element formulation based on the ELD can lead to moving-grid finite element procedure, which is very efficient for modeling the geometry change. In specific, the method has been successfully applied to various fracture problems.

A special static, small-deformation form of the ELD was used to develop finite element procedure for computing the stress intensity factors in linear elastic fracture problems [11, 12]. Since the ELD model allows a geometric variation to represent a true virtual crack extension, a true variational formulation of the explicit expressions for the mutual potential energy release rates is possible. The instantaneous energy release rates are evaluated directly from integral expressions defined over quarter-point singular isoparametric elements. Results of application to several pure mode-I and mixed-mode problems prove that the method produces very accurate results, even for a relatively coarse mesh and for an integration domain close to the crack tip.

The small-deformation of the ELD was extended to elastodynamic problems, specially to the analysis of dynamic crack propagation problems [6, 7]. A special weak form of the variational equations of motion was derived, and used for the basis of finite element formulation using moving-grid procedure [6]. The moving-grid method was successfully applied to the analysis of dynamic crack propagation problems [7]. The convective terms in the dynamic ELD model, in conjunction with singular quarter-point isoparametric elements, produce the proper singular forms in both the stress and material velocity fields. There is no need to use special non-confirming singular elements, as with conventional Lagrangian finite element models. The mesh motion due to crack growth is introduced in continuous form, so there is no need to remesh locally and interpolate field variables as in Lagrangian remeshing procedures.

Recently, a mixed variational statement based on the ELD has been proposed by Lee [13] for the analysis of crack growth in creeping materials. Lee showed that the moving-grid method based on the ELD is able to model crack growth in history-dependent materials very accurately and effectively [13].

The dynamic ELD model was also applied to the prediction procedure for dynamic crack propagation and arrest problems [8]. The procedure utilizes the false method : the variational statement of the equation of motion and the energy balance equation, a fracture criterion, are solved separately for the displacement field and crack-tip velocity, respectively, with the fixed crack-tip velocity and the displacement field. The method is simple to use, since there is little need to modify the previous solution procedure for the analysis type problems. However, fully incremental expressions of the nonlinear governing equations which are suitable for the Newton type solution procedure were not derived. This paper presents an incremental formulation of the ELD moving-grid finite element method which can predict both field variables and crack-tip velocity simultaneously by using a Newton type solution procedure.

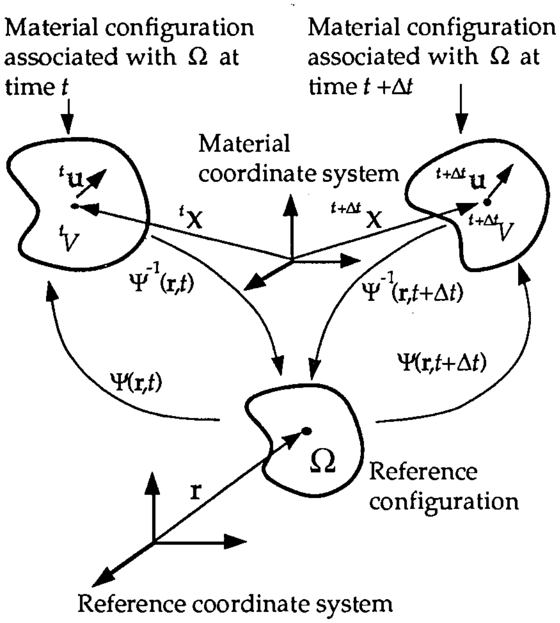

a) Small deformation kinematic model

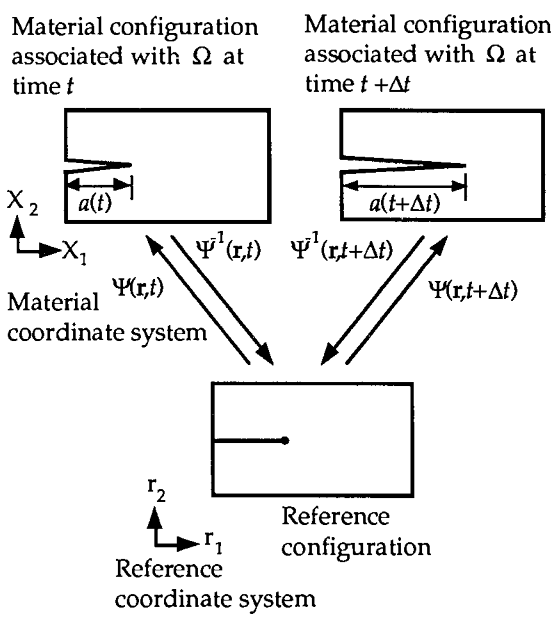

b) Kinematic model for two-dimensional fracture problems

Figure 1. The Eulerian-Lagrangian kinematic model for small deformation problems

3. INCREMENTAL FORMULATION FOR PREDICTION PROBLEMS

3.1 The variational statement of the equation of motion

In fracture problems, the material configuration changes with crack growth (Fig. 1b). A time-dependent mapping Ψ, from the reference configuration to the material configuration, is introduced to describe changes of material configuration caused by crack growth.

$$\mathbf{X} = \Psi(\mathbf{r}, a(t)) \tag{1}$$

where $a(t)$ is crack-tip motion. Material and referential time derivatives are evaluated with fixed material coordinates $\mathbf{X}$ and reference coordinates $\mathbf{r}$, respectively. The referential and material time derivatives are related by the following equation [6].

$$\dot{(\ )} = \overset{*}{(\ )} + \nabla(\ )\cdot\dot{\mathbf{X}} = \overset{*}{(\ )} + \nabla_r(\ )\cdot\bar{\mathbf{J}}\cdot\dot{\mathbf{X}} \tag{2}$$

where superposed * and $^\bullet$ denote material and referential time derivative operators. $\bar{\mathbf{J}}$ is the inverse Jacobian of the geometric mapping; and ∇ and ∇_r are the gradient operators with respect to $\mathbf{X}$ and $\mathbf{r}$.

The variational statement of the equation of motion for the elastodynamic problems, written in the reference configuration, was presented by Koh and Haber [6]. In case that material motion is not allowed across the physical boundaries of the given material volume and that the geometric mapping changes only in X_1 direction, the variational statement of the equation of motion is given as follows.

$$\begin{aligned} F(\hat{\mathbf{u}}, \mathbf{u}, a, \Omega) \equiv & \int_\Omega (\nabla_r\hat{\mathbf{u}}\cdot\bar{\mathbf{J}}):\mathbf{C}:(\nabla_r\mathbf{u}\cdot\bar{\mathbf{J}})\tilde{J}d\Omega - \int_\Omega \hat{\mathbf{u}}\cdot\mathbf{b}\tilde{J}d\Omega - \int_{\Gamma_t}\hat{\mathbf{u}}\cdot\bar{\mathbf{T}}K_a d\Gamma \\ & + \int_\Omega \rho\hat{\mathbf{u}}\cdot\ddot{\mathbf{u}}\tilde{J}d\Omega - 2\int_\Omega \rho\hat{\mathbf{u}}\cdot\nabla_r\dot{\mathbf{u}}\cdot\bar{\mathbf{J}}\cdot\dot{\mathbf{X}}\tilde{J}d\Omega - \int_\Omega \rho\hat{\mathbf{u}}\cdot\nabla_r\mathbf{u}\cdot\bar{\mathbf{J}}\cdot\ddot{\mathbf{X}}\tilde{J}d\Omega \\ & - \int_\Omega \rho(\nabla_r\hat{\mathbf{u}}\cdot\bar{\mathbf{J}}\cdot\dot{\mathbf{X}})\cdot(\nabla_r\mathbf{u}\cdot\bar{\mathbf{J}}\cdot\dot{\mathbf{X}})\tilde{J}d\Omega = 0 \qquad \forall\hat{\mathbf{u}}\in\mathcal{V}_{\hat{\mathbf{u}}} \end{aligned} \tag{3}$$

where $\mathbf{u}\in\mathcal{V}_\mathbf{u}$ and the following definitions of function spaces apply.

$$\mathcal{V}_\mathbf{u} \equiv \{\mathbf{u}\in H^1(\Omega) \mid \mathbf{u} = \bar{\mathbf{u}} \text{ on } \Gamma_u\times]0,T[\,\}, \quad \mathcal{V}_{\hat{\mathbf{u}}} \equiv \{\hat{\mathbf{u}}\in H^1(\Omega) \mid \hat{\mathbf{u}} = 0 \text{ on } \Gamma_u\} \tag{4}$$

Here, Γ_t and Γ_u are surface regions of the reference volume on which displacements and tractions are prescribed. ρ, $\mathbf{b}$, $\mathbf{C}$, $\bar{\mathbf{u}}$, $\bar{\mathbf{T}}$, $\tilde{J}$ and K_a are, respectively, the mass density, the body force vector, the elasticity tensor, prescribed displacements, prescribed tractions, the determinant of the Jacobian, and area metric. $H^1(\Omega)$ denotes the Sobolev space of degree one on Ω. Initial conditions for the equation of motion are

$$\mathbf{u}(\mathbf{X},0) = {}^0\mathbf{u}(\mathbf{X}), \quad \overset{*}{\mathbf{u}}(\mathbf{X},0) = {}^0\overset{*}{\mathbf{u}}(\mathbf{X}) \tag{5}$$

3.2 Energy balance equation

A proper fracture criterion should be selected to define crack-tip motion. The energy balance criterion is employed for the elastodynamic fracture criterion in this study. The energy balance criterion is expressed as

$$G \equiv \frac{d}{dB}(W-T-\Phi)=\frac{d}{\dot{a}sdt}(W-T-\Phi)=R \tag{6}$$

where G, W, T, Φ, B, $\dot{a}$, s and R are dynamic energy release rate, external work, kinetic energy, strain energy, traction free surface generated by crack growth, crack-tip velocity, the plate thickness in two-dimensional problems and the fracture energy, respectively.

The fracture energy R for pure mode-I crack propagation is expressed in terms of the dynamic fracture toughness through the Freund-Nilsson's function $f(\dot{a})$ [2].

$$R=\frac{1}{2\mu}f(\dot{a})K_{ID}^2 \tag{7}$$

where μ, $f(\dot{a})$ and K_{ID} are the shear modulus, a crack-tip velocity-dependent function and the dynamic fracture toughness. The dynamic fracture toughness K_{ID} is assumed to be a material property that depends on only crack-tip velocity, and is determined by experiments.

Equation (6) requires initial conditions for $\mathbf{u}$ and a since W, T and Φ are implicit functions of $\mathbf{u}$, $\dot{\mathbf{u}}$, a and $\dot{a}$. Therefore, in addition to (5), initial conditions for a should be specified.

$$a(0)={}^0a\,,\quad \dot{a}(0)={}^0\dot{a} \tag{8}$$

The energy balance equation is obtained by integrating equation (6) from the initial time 0 to the current time t.

$$E_b(\mathbf{u},\ a,\ \Omega)={}^tW-{}^tT-{}^t\Phi-({}^0W-{}^0T-{}^0\Phi)-\int_0^t R(\dot{a})\dot{a}s\,d\tau=0 \tag{9}$$

The term in the parentheses of equation (9) vanishes if crack is stationary at time 0. Equation (9) states that the change in the total potential energy is equal to the work done by the crack resistance force during crack growth. The solution for the prediction problem of dynamic crack propagation is obtained by solving the variational statement of the equation of motion (3) and the energy balance equation (9) simultaneously for the displacement and the crack-tip motion.

3.3 Incremental formulation

The incremental formulation of equations (3) and (9) begins with time discretization. It is assumed that all of the field variables are known at the end of the previous time step, time t, and that crack is stationary at time 0. The variational statement of the equation of motion and the energy balance equation at time $t+\Delta t$ are

$${}^{t+\Delta t}F \equiv F(\hat{\mathbf{u}},\ {}^{t+\Delta t}\mathbf{u},\ {}^{t+\Delta t}a,\ \Omega)=0 \qquad \forall\hat{\mathbf{u}}\in\mathcal{V}_{\hat{\mathbf{u}}} \tag{10}$$

$${}^{t+\Delta t}E_b \equiv E_b\ ({}^{t+\Delta t}\mathbf{u},\ {}^{t+\Delta t}a,\ \Omega)\ ={}^{t+\Delta t}W-{}^{t+\Delta t}T-{}^{t+\Delta t}\Phi-\int_0^{t+\Delta t}R(\dot{a})\dot{a}s\,d\tau=0 \tag{11}$$

where ${}^{t+\Delta t}\mathbf{u}\in\mathcal{V}_{{}^{t+\Delta t}\mathbf{u}}$. The function space for $\hat{\mathbf{u}}$ is given by equation (4), and

$$\mathcal{V}_{^{t+\Delta t}\mathbf{u}} \equiv \{ {}^{t+\Delta t}\mathbf{u} \in H^1(\Omega) \mid {}^{t+\Delta t}\mathbf{u} = {}^{t+\Delta t}\bar{\mathbf{u}} \ \text{on}\, \Gamma_u \} \tag{12}$$

The generalized midpoint rule is applied to the time integral in equation (11).

$$\int_0^{t+\Delta t} R\dot{a}s d\tau = \int_0^{t} R\dot{a}s d\tau + \int_t^{t+\Delta t} R\dot{a}s d\tau \approx \int_0^{t} R\dot{a}s d\tau + {}^{t+\alpha\Delta t}(R\dot{a})s\Delta t \tag{13}$$

where α is a specified integration parameter within the range 0 to 1, and

$${}^{t+\alpha\Delta t}(R\dot{a}) = {}^{t+\alpha\Delta t}R\, {}^{t+\alpha\Delta t}\dot{a}$$

$${}^{t+\alpha\Delta t}R = R\,({}^{t+\alpha\Delta t}\dot{a}) \quad , \quad {}^{t+\alpha\Delta t}\dot{a} = (1-\alpha)\,{}^{t}\dot{a} + \alpha\,{}^{t+\Delta t}\dot{a}$$

Substitution of equation (13) into equation (11) leads to the following expression.

$${}^{t+\Delta t}E_b \approx {}^{t+\Delta t}W - {}^{t+\Delta t}T - {}^{t+\Delta t}\Phi - \int_0^{t} R\dot{a}s d\tau - {}^{t+\alpha\Delta t}(R\dot{a})s\Delta t = 0 \tag{14}$$

Equations (10) and (14) are discretized by employing isoparametric finite element models. In the isoparametric specialization of the ELD, a mapping is established between a parent element domain and an actual material domain. The parent element domain serves as the fixed, local reference domain. A more complete development of isoparametric finite element method for the elastodynamic ELD was presented by Koh and Haber [6]. In the isoparametric finite element models, motion of the finite element mesh in the material domain is represented by changes of nodal coordinates which can be related to crack-tip motion by auxiliary regional mappings [7]. With this auxiliary mappings, we can express mesh motion $\mathbf{X}$ and its referential time derivatives with respect to the crack-tip motion a and its time derivatives.

3.4 Iteration solution strategy

An iterative scheme is necessary to solve (10) and (14) simultaneously for the displacement and the crack-tip motion at time $t+\Delta t$. Two nested sets of iteration are employed within each time step. The outer iterations are used to satisfy the variational statement of equation of motion (10) and the inner iterations are used to satisfy the energy balance equation (14) under fixed displacements. Hereafter, the outer iterations and the inner iterations are referred to as the equilibrium iterations and the energy iterations, respectively.

3.4.1 *The equilibrium iteration* The iteration updates of the displacement and the crack-tip motion are defined as follows.

$${}^{t+\Delta t}\mathbf{u}_i = {}^{t+\Delta t}\mathbf{u}_{i-1} + \Delta\mathbf{u} \qquad {}^{t+\Delta t}a_i = {}^{t+\Delta t}a_{i-1} + \Delta a \tag{15}$$

where the right subscript i denotes the iteration count and Δ indicates an iteration increment. The notation $(\ )_0$ indicates the initial estimate of $(\ )$ at time $t+\Delta t$. It is assumed that all of the field variables from $(i\text{-}1)$-th iteration are available and that previous estimate of the solution satisfies (14), but does not satisfy (10). The iteration update of geometry changes of material domain, $\Delta\mathbf{X}$, is expressed in terms of Δa.

$$\Delta\mathbf{X} = \frac{\partial\Psi}{\partial a}\Delta a \tag{16}$$

The iteration increments for the inverse Jacobian and the determinant of Jacobian [6] are given by

$$\Delta \bar{\mathbf{J}} = -\underline{\bar{\mathbf{J}}} \cdot \Delta \mathbf{X} \cdot \underline{\bar{\mathbf{J}}} + \text{H.O.T.} \tag{17}$$

$$\Delta \tilde{J} = e_{jkl}(\Delta \tilde{J}_{j1} \underline{\tilde{J}}_{k2} \underline{\tilde{J}}_{l3} + \underline{\tilde{J}}_{j1} \Delta \tilde{J}_{k2} \underline{\tilde{J}}_{l3} + \underline{\tilde{J}}_{j1} \underline{\tilde{J}}_{k2} \Delta \tilde{J}_{l3}) + \text{H.O.T.} \tag{18}$$

where e_{jkl} and $\tilde{J}_{ij}$ are, respectively, the permutation symbol and Jacobian components, and repeated subscripts in equation (18) imply summation. The underlined variables in equation (17) and (18) are evaluated using the solutions of the previous iteration. The increment of Jacobian components is

$$\Delta \tilde{J}_{ij} = \frac{\partial \Delta X_i}{\partial r_j} \tag{19}$$

A truncated Taylor expansion of ${}^{t+\alpha\Delta t}(R\dot{a})$ appearing in (14), yields

$${}^{t+\alpha\Delta t}(R\dot{a})_i = {}^{t+\alpha\Delta t}(R\dot{a})_{i-1} + \alpha\, {}^{t+\alpha\Delta t}(R\dot{a})'_{i-1} \Delta \dot{a}_i \tag{20}$$

where

$${}^{t+\alpha\Delta t}(R\dot{a})'_{i-1} = \left.\frac{\partial R\dot{a}}{\partial \dot{a}}\right|_{\dot{a} = {}^{t+\alpha\Delta t}\dot{a}}$$

The linearized, iterative forms of the variational statement of equation of motion and the energy balance equation with respect to $\Delta\mathbf{u}$, Δa and their referential time derivatives are obtained by substituting (15), (17), (18) and (20) into (10) and (14) and including only first order terms in incremental expressions [9]. To approximate the first- and second order referential time derivatives of the displacement and the crack-tip motion, the Newmark β-method is employed.

3.4.2 *Energy iteration* The solutions obtained by equilibrium iterations do not satisfy the energy balance equation exactly since the crack-tip motion is estimated by the linearized energy balance equation. The crack-tip motion that are consistent with the displacement field obtained in the equilibrium iteration and that satisfy the energy balance equation (14) is computed by applying additional iteration procedure to equation (14) under the fixed displacement within each equilibrium iteration. The incremental form of the energy balance equation (14) for the energy iteration is easily derived by considering the iteration update of the crack-tip motion only.

The convergence rate of overall solution procedures is accelerated by the energy iteration. Additional computational costs required for the energy iteration are relatively cheap because there is only one unknown - crack-tip motion - in the energy iteration. Therefore, total computational coats are reduced by employing the energy iteration.

4. NUMERICAL EXAMPLES AND DISCUSSIONS

The proposed method is applied to the prediction problem of mode-I dynamic crack propagation in five wedge-loaded rectangular double cantilever beam (RDCB) specimens under plain stress condition. The dimensions of the RDCB specimens are the same as those used in experiments performed by Kalthoff *et al* [4]. In their

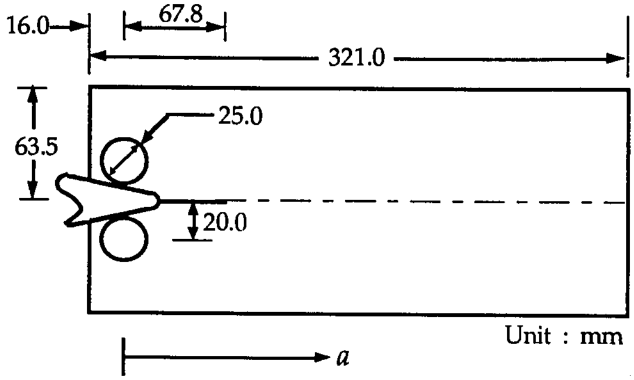

Dynamic Material Properties

E = 3660 MPa
ν = 0.39
ρ = 1172 Kg/m ^{3}
Shear wave speed = 1060 m/sec
Dilatational wave speed = 1920 m/sec
Initial Crack Length, a_0 = 67.8 mm

Figure 2 RDCB specimen of Kalthoff *et al*

experiments, the crack tip was initially blunted. The value of the crack initiation stress intensity factor (SIF), K_{IQ}, depends on the degree of blunting. The specimens with K_{IQ} values of 2.32 MPa-m$^{0.5}$, 1.76 MPa-m$^{0.5}$, 1.33 MPa-m$^{0.5}$, 1.03 MPa-m$^{0.5}$ and 0.74 MPa-m$^{0.5}$ are referred as RDCB-4, RDCB-8, RDCB-17, RDCB-24 and RDCB-62, respectively [4]. All of the five specimens have the same dimensions and material properties, which are shown in Fig. 2. The dynamic fracture toughness data measured experimentally by Kalthoff *et al* [4] are used, and are shown in Fig. 3 by a solid line. Because the experimentally measured dynamic fracture toughness data are available up to the crack-tip velocity of about 340 m/sec, the dynamic fracture toughness data for the crack-tip velocity greater than 340 m/sec are generated by extrapolating the experimentally measured dynamic fracture toughness data by a quadratic parabola. The extrapolated dynamic fracture toughness data are illustrated by a dashed line in Fig. 3.

The loading condition is modeled by prescribing a displacement at the pin location. The prescribed displacement is increased until the static SIF reaches to the crack initiation SIF, K_{IQ}, and thereafter maintained constantly throughout the prediction calculation. Due to symmetry, only the upper half of the specimen is modeled by finite elements. The finite element mesh contains 1536 LST elements and

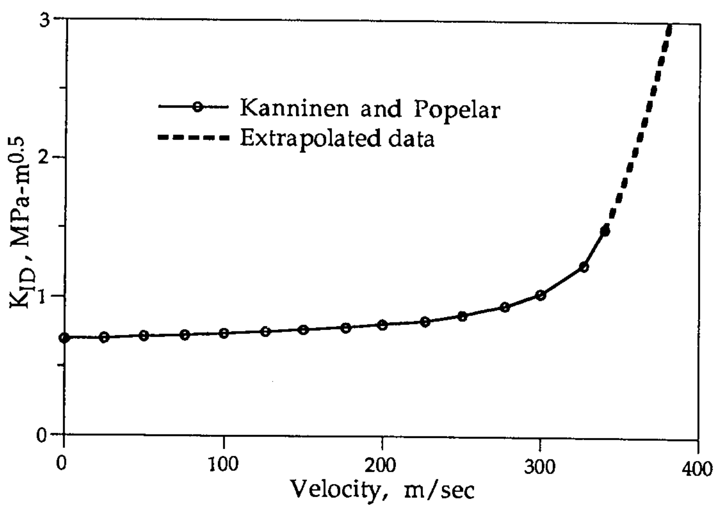

Figure 3.
Dynamic fracture toughness data by Kalthoff *et al* [4].

3225 nodes. The singularity in the strain field is modeled by using four triangular quarter-point isoparametric crack-tip elements, which also introduce the singularity of the material velocity field through the inverse Jacobian components in equation (2) [7].

The integration constant for the generalized midpoint rule, $\alpha = 0.5$ is used, unless stated otherwise. The Newmark's parameters, $\delta = 0.5$ and $\beta = 0.25$ are constant throughout the prediction procedures. A nonuniform time increment is used (0.5 μsec up to the second time step, 1 μsec up to twenty second time step, 1.5 μsec up to twenty fourth time step and 3 μsec thereafter).

The effects of the crack-tip acceleration on the crack-tip motion are neglected because the crack tip has no inertia [5]. This means that the crack-tip acceleration has no effect on changes in the crack-tip velocity. Thus, the term that contains the crack-tip acceleration in equation (3) is dropped.

A suitable initial condition should be specified to initiate a stationary crack in the present method. The initial condition can be given by specifying either initial crack-tip velocity or a small increment of the prescribed displacement at the pin location. Three different initial conditions are tried; ${}^{0}\dot{a} = 0.0066\ C_s$, ${}^{0}\dot{a} = 0.05\ C_s$ and $\Delta \mathbf{u}_p = 0.0001\bar{\mathbf{u}}$. Here, C_s and $\bar{\mathbf{u}}$ are the shear wave speed and the prescribed displacement at the pin location. The three initial conditions yield almost identical results (see Fig. 8). Since an increment of the prescribed displacement at the pin location may produce artificial stress waves, results by the first initial condition(${}^{0}\dot{a} = 0.0066\ C_s$ and $\Delta \mathbf{u}_p = 0.0001\bar{\mathbf{u}}$) are presented hereafter, unless specified otherwise.

Fig. 4 and Fig. 5 show the results for the crack length versus time and the dynamic stress intensity factor versus the crack length predicted by the present method, respectively. The crack length predicted by the present method is almost identical to the experimental results by Kalthoff *et al* [4]. The dynamic SIF predicted by the present method agrees very well with the experimental results of Kalthoff *et al* [4]. The experimental results at early times are not available to authors as yet. The crack arrests a little earlier for RDCB-4 and RDCB-8, and a little later for RDCB-24 and RDCB-62 in the present method than in the experiment. The crack arrest

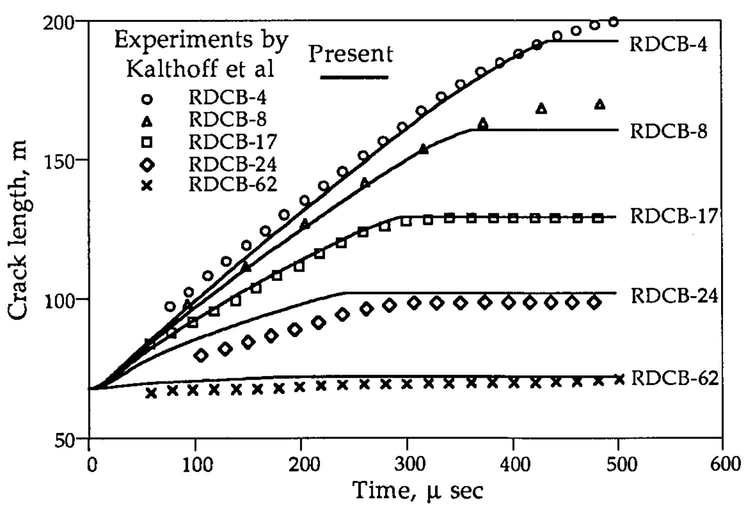

Figure 4.
Crack-length for various specimens

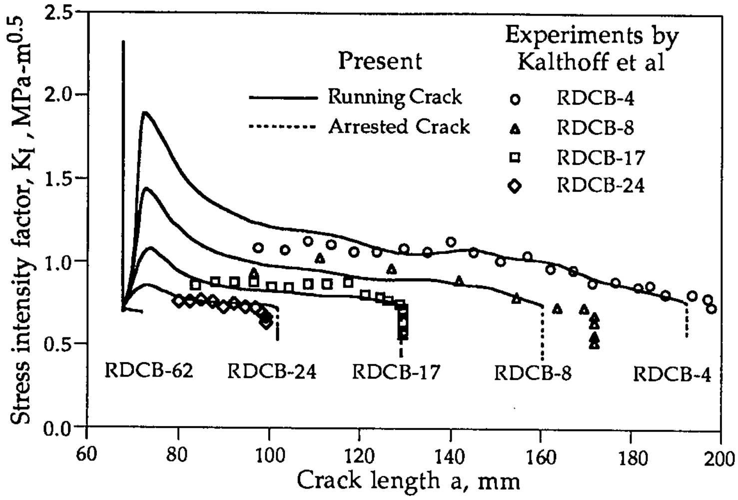

Figure 5.
Stress intensity factors for various specimens

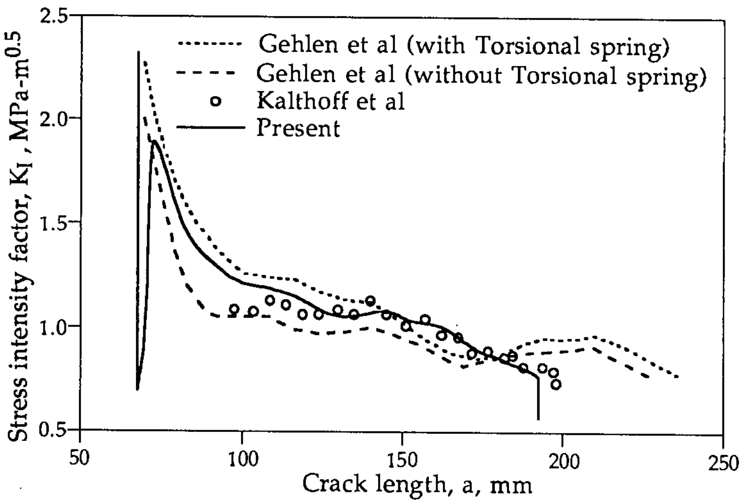

Figure 6.
Stress intensity factors for RDCB-4

time and crack length predicted by the present method for RDCB-17 are almost identical to the experimental results. The results for RDCB-4 reported by Gehlen [3], based on one-dimensional, double cantilever beam formulation, also appear in Fig. 6 for comparison. In Fig. 6, a transient period is clearly seen for RDCB-4 just after crack starts to grow by the present method.

The crack-tip velocity history are shown Fig. 7. The crack-tip velocity reaches to the maximum values after a short transient period. The crack arrests at 438 μsec for RDCB-4, 366 μsec for RDCB-8, 298 μsec for RDCB-17, 246 μsec for RDCB-24 and 195 μsec for RDCB-62. Crack arrest occurs abruptly in all specimens, which agrees with Kanninen and Popelar's argument that crack arrests abruptly at a value that is unrelated to the corresponding static conditions [5].

As mentioned earlier, a short transient period exists just after crack starts propagating. Fig. 8 shows the dynamic SIF for RDCB-4 during the transient period for the three different initial conditions. The dynamic SIF is instantly reduced from the initiation SIF, K_{IQ}, to about minimum value of the dynamic fracture toughness, $(K_{ID})_{min}$ immediately after the crack begins to grow. This phenomenon can be explained as follows. Since the crack-tip is blunted initially, the initiation SIF K_{IQ}, is larger than K_{ID} (0). However, just after the crack starts to grow, the dynamic SIF becomes the dynamic fracture toughness value corresponding to the current crack-tip velocity. After the crack initiation, the dynamic SIF increases very rapidly as crack-tip velocity becomes faster.

The finite element solutions by the present method show good agreement with experimental results. The proposed iterative solution procedures converge rapidly within 2 or 3 iterations. The present method can provide a very stable and accurate numerical scheme in investigating behaviors of dynamically growing crack in brittle materials

ACKNOWLEDGEMENT

This research was supported by Korea Science and Engineering Foundation during 1988-1990. The authors are grateful to Cray Research Inc. for providing access to Cray 2-S/4-128 supercomputer at the Systems Engineering Research Institute, Korea Institute of Science and Technology through the University Research & Development Grant Program.

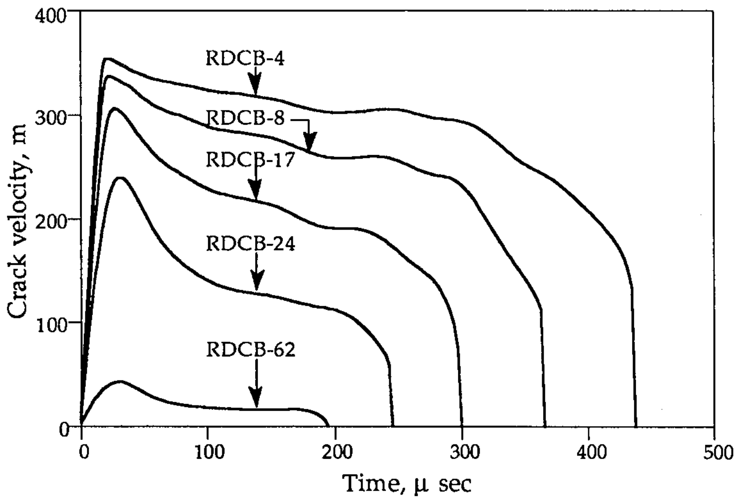

Figure 7
History of crack-tip velocity of various specimens

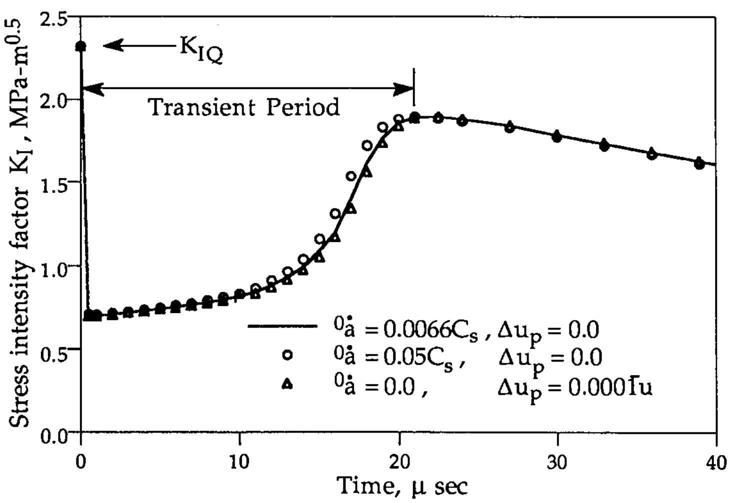

Figure 8
Initiation behavior of RDCB-4 for different initial conditions

REFERENCES

1. Atluri, S. N. and Nishioka, T. 1985. Numerical studies in Dynamic Fracture Mechanics. *International Journal of Fracture,* vol. 27. pp. 245-261.
2. Freund, L. B. 1972. Energy Flux into the tip of an Extending Crack in an Elastic Solid. *Journal of Elasticity,* vol. 2. pp. 341-349.
3. Gehlen, P. C., Popelar, C. H. and Kanninen, M. F. 1979. Modeling of Dynamic Crack Propagation: I. Validation of One-dimensional Analysis. *International Journal of Fracture,* vol. 15, no. 3. pp. 281-294.
4. Kalthoff, J. F., Beinert, J., Winkler, S. 1977. Measurements of Dynamic Stress Intensity Factors for Fast Running and Arresting Cracks in Double-Cantilever-Beam Specimens. in *Fast Fracture and Crack Arrest, ASTM STP 627.* ed. by Hahn, G. T. and Kanninen, M. F. pp. 161-176, Philadelphia. American Society for Testing and Materials.
5. Kanninen, M. F. and Popelar, C. H. 1985. *Advanced Fracture Mechanics.* New York: Oxford University Press.
6. Koh, H. M. and Haber, R. B. 1986. Elastodynamic Formulation of the Eulerian-Lagrangian Kinematic Description. *Journal of Applied Mechanics,* vol. 53. pp. 839-845.
7. Koh, H. M., Lee, H. S. and Haber, R. B. 1988. Dynamic Crack Propagation Analysis Using Eulerian-Lagrangian Kinematic Descriptions. *Computational Mechanics,* vol. 3, pp. 141-155.
8. Koh, H. M. and Yun, C. H. 1991. Prediction of Dynamic Crack Propagation and Arrest by Moving Finite Element Method. *Transaction of SMiRT 11, Vol. G.* pp. 261-266.
9. Koh, H. M. and Kim, M. H. 1992. Numerical Procedure for the Prediction of Dynamic Fracture/Computer Graphics Pre- and Post-Processing. *Final Report of Cray Sponsored Research.*
10. Haber, R. B. 1984. A Mixed Eulerian-Lagrangian Displacement model for Large-Deformation Analysis in Solid Mechanics. *Computer Methods in Applied Mechanics and Engineering,* vol. 43. pp 127-143.
11. Haber, R. B. and Koh, H. M. 1984. An Eulerian-Lagrangian Virtual Crack Extension Method for Mixed mode Fracture Problems. *Proceedings of the 25th Structures, Structural Dynamics and Material Conference, AIAA/ASMEASCE/ AHS, Part I, Palm Springs, CA.* pp. 116-122.
12. Haber, R. B. and Koh, H. M. 1985. Explicit Expressions for Energy Release Rates Using Virtual Crack Extensions. *International Journal for Numerical Methods in Engineering,* vol 21. pp. 301-315.
13. Lee, H. S. 1991. An Eulerian-Lagrangian Finite Element Method for Modeling Crack Growth in Creeping Materials. *Ph.D. Thesis,* Department of Civil Engineering, University of Illinois at Urbana-Champaign.
14. Swenson, D. V. and Ingraffea, A. R. 1988. Modeling Mixed-mode Dynamic Crack Propagation Using Finite Element Theory and Applications. *Computational Mechanics,* vol. 3, pp. 381-397.
15. Caldis, E. S., Owen, D. R. J. and Zienkiewicz, O. C. 1979. Nonlinear Dynamic Transient Methods in Crack Propagation Studies. *Nonlinear Mechanics, AMD,* vol. 35 pp. 1-17.